Dendrite Growth Model in Battery Cell Combining Electrode Edge Effects and Stochastic Forces into a Diffusion Limited Aggregation Scheme

Roberto Failla[a], Mauro Bologna[b], Bernardo Tellini[c,*]

[a]*Center for Nonlinear Science, University of North Texas, Denton, TX 76203, USA.*
[b]*Instituto de Alta Investigación, Universidad de Tarapacá, Arica, Chile.*
[c]*Dipartimento di Ingegneria dell'Energia, dei Sistemi, del Territorio e delle Costruzioni, Largo Lucio Lazzarino, I-56122, Pisa, Italy.*

Abstract

In this paper, we present a new model of dendrite growth in battery cells through theoretical and numerical analysis. We use a statistical model based on the competition between a deterministic electric field and a stochastic force, which both drive the movement of the particles inside the battery cell. The simulation of the dendrite growth is modeled via Diffusion Limited Aggregation. As a major aspect, we point out the key role played by the intense electric field close to the edges of the electrodes, which statistically drives the particles along the electric field lines.

Keywords: `Dendrite Formation`, Diffusion Growth, Electrode Edge Effect, Statistical model

1. Introduction

Dendrite growth represents a major aspect for the success of lithium batteries technology, and a complete and comprehensive model is still under investigation. Among the various factors, temperature, electrolyte nature, and nonuniform current distribution on the electrode surface jointly are at the basis of dendrite

*Corresponding author

Email addresses: rf0009@att.net (Roberto Failla), mauroh69@gmail.com (Mauro Bologna), bernardo.tellini@unipi.it (Bernardo Tellini)

formation [1]. However, it is recognized that high current densities are the cause of dendrite growth [2], [3], [4].

Several papers focus on the effect of electric field distribution on the dendrite growth [2], [5], [6], and [7]. Cui *et al.* experimentally analyze the effect of an external electric field in the formation of dendritic carbon nanotubes in acid solution, and they clearly show the influence of an external electric field. Jana *et al.* investigate the effect of the separator pore size on the dendrite growth through a phase field method. Concerning the electric field, the authors conclude that an inhomogeneous electric field distribution increases the deposition rate, thus improving the dendrite growth. Kong *et al.* develop a lithium cell consisting of two lithium electrodes and a liquid electrolyte. They provide experimental evidence of dendrite formation at the corner of the electrodes where the electric field intensity is higher. Zou *et al.* consider the electric field distribution as a dominant factor and propose a copper grid to be interposed between the electrodes, in order to modify the direction of the electric field force lines. Through such a grid, the authors demonstrate that dendrites are guided to grow parallel to the electrode plates, thus increasing the safety of the cell.

In [8], Rezinkina presents a model to study the shape of dendrite growth as a function of the electric field. In more detail, the model divides the domain of interest in conducting and insulating regions, and assumes a stochastic process for which the probability to change from one region to the other is determined by the electric field intensity. The conclusion of his work, indicates dendrite branching mainly in the longitudinal direction, while this effect diminishes for lower voltages.

In [9], Aryanfar *et al.* analyze the effect of pulse charging through a Monte Carlo calculation. The authors show that shorter charge pulses mitigate the dendrite growth, although their duration has to be larger than some characteristic time. In addition, they also demonstrate how an appropriate frequency rate can contribute to the reduction of the dendrite formation.

We start our analysis again analytically deriving the electric field distribution for a capacitor made by two disk electrodes. Indeed, the charge distribution and the electric field are not uniform on the electrode surface and ideally diverge at the edges. Thus, our conjecture is that such regions are particularly critical for the dendrite growth.

Park *et al*. propose a relatively stable electrolyte system with respect to lithium metal and able to reduce the dendrite growth, combining simulation with *in situ* experimental observation [10]. In particular, the effect of the viscosity of the electrolyte is analyzed through a Diffusion Limited Aggregation (DLA) simulation model [11]. In [12], the fractal shape of dendrites forming during electrodeposition is simulated by a DLA method, although the authors state how there is still lack to predict shape and proper time scale for a real case. In order to explore our conjecture, we also implement the effect of a nonuniform driving force into a DLA scheme based on Brownian motion. The computation domain is subdivided into several regions of probability and the results of this simulation are then compared with the case of uniform driving force.

Analyses by Scanning Electron Microscopy of the electrode morphology shows a rough surface. Within this context, whenever the radius of curvature of the asperity peaks is relatively small, high intensity electric fields are expected, but, as it will be better discussed throughout the paper, such local fields are expected to vanish at a relatively short distance. Thus, on average, the electric field distribution inside the capacitor will not be affected by these local fields, but rather by the edge effects, which are expected to play a key role on a relatively long distance.

The paper is organized as follows: In Sec. 2, we reformulate the classical electrostatic problem of the charge distribution on a parallel plate capacitor with disk electrode of finite radius, and point out the edge effects. In Sec. 3, we present a statistical model combining the deterministic electric force with a stochastic force due to the collision among all the particles inside the cell. The model shows that the probability to find a charged particle (ion) in a given region of the battery cell is determined by the electric potential and ultimately by the electric field. In Sec. 4, we propose a simulation model based on a DLA scheme. For each simulation, we follow the movement of one single charged particle driven by a stochastic force due to the interaction with all the particles inside the cell, and a deterministic force due to the electric field. The stochastic force generates a diffusion process and competes with the deterministic force. The numerical analysis reproduces the growth of dendrites along the field lines, which are denser close to the ends of the cell. Finally, in Sec. 5 we draw our conclusions.

2. Finite Capacitor Model

An accurate analysis of the electrostatic potential distribution inside a battery cell is a complex task. At a first approximation, the electric field generated within the double layer at the interface electrode/electrolyte can be assumed uniform and to decay abruptly immediately outside. More advanced models simulate a gradual transition of the electric field across a diffused double layer [13].

Under the hypothesis of electrodes with relatively high electrical conductivity with respect to the electrolyte, we can assume the charge relaxation time on the electrode surface negligible, and finally define an electrostatic problem to investigate the electric field in the electrolyte, during the charge and discharge phases. As a matter of fact, an electrostatic field $\mathbf{E}$ moves the ions across the electrolyte, and in the electrolyte solution holds the Ohm's law $\mathbf{J} = \sigma\mathbf{E}$, where $\mathbf{J}$ and σ are the local current density and electrical conductivity. Knowing the charge distribution at the electrodes, we could finally solve the electrostatic problem and determine the electric field distribution into the cell.

Here, we derive the charge and field distributions for a two-parallel disk capacitor, showing how the electric field intensity diverges at the very electrode edge region. Our conjecture aims at discussing how edge effects can play an important role in the dendrite formation. Relatively more intense field values are expected close to the electrode edges in the actual case, thus making such regions more critical for the growth of dendrites.

The evaluation of the electric field distribution between two parallel disks is

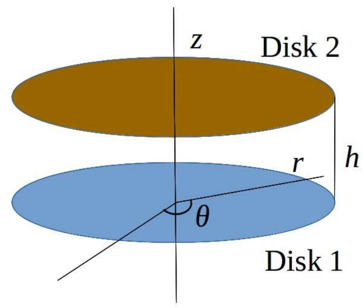

Figure 1: Two disk capacitor scheme.

a known problem of electrostatics and it can be found in the classical literature [14]. This appears also in the study of current density distribution for battery cell as well as for electrodeposition problems [15], [16]. Recently, some papers provided experimental evidences on how edges and corners are preferential spots for dendrite growth [2], [17], [18]. Although an accurate modeling is still missing, we believe this discussion can contribute to shed some more light on this specific issue.

Let us consider the very basic case of the electric field distribution inside a finite capacitor. The anode and cathode are in our case modeled as two disks of finite radius a. In order to simplify the calculation for the potential of a disk of radius a we will use a more handy expression than the one used in [14]. We introduce the polar coordinate system (r, θ, z) and we set the origin of the reference frame at the center of the bottom disk, as shown in Fig. 1. The electric potential generated by the two disks has the following expression:

$$\varphi_1(r,z) = \frac{2V_1}{\pi} \times \sin^{-1}\left[\frac{2a}{\sqrt{(r-a)^2+z^2}+\sqrt{(r+a)^2+z^2}}\right], \tag{1}$$

$$\varphi_2(r,z) = \frac{2V_2}{\pi} \times \sin^{-1}\left[\frac{2a}{\sqrt{(r-a)^2+z_1^2}+\sqrt{(r+a)^2+z_1^2}}\right]. \tag{2}$$

where $\varphi_1(r,z)$ and $\varphi_2(r,z)$ are the electric potentials generated by the bottom and the upper disk, respectively, and h is the distance between the two disks. Also, we introduced $z_1 = z - h$ for more compact notation. The electric field is given by

$$\mathbf{E} = -\nabla\varphi(r,z), \quad \varphi(r,z) = \varphi_1(r,z) - \varphi_2(r,z). \tag{3}$$

We omit the exact expression for $\mathbf{E}$ since it is quite large. We will focus on the central region and on the circular boundaries. The field in the central region of the capacitor ($r \ll a$) at first non-vanishing order r/a is given by

$$\begin{aligned} E_r(r,z) &\approx 0, && (4)\\ E_\theta(r,z) &= 0, && (5)\\ E_z(r,z) &\approx \frac{2V}{\pi a}\left[\frac{1}{\left(1+\left(\frac{h-z}{a}\right)^2\right)} + \frac{1}{\left(1+\left(\frac{z}{a}\right)^2\right)}\right]. && (6)\end{aligned}$$

Near $r \approx a$ we have

$$\begin{aligned} &E_r(r,z) \approx \frac{4\sqrt{2}V}{\pi a}\\ &\left[\frac{1}{\sqrt{\frac{z}{a}}\sqrt{\left(\frac{z}{a}\right)^2+4}\left(\frac{z}{a}+\sqrt{\left(\frac{z}{a}\right)^2+4}\right)^{3/2}}+\right.\\ &\left.-\frac{1}{\sqrt{\frac{h-z}{a}}\sqrt{\left(\frac{h-z}{a}\right)^2+4}\left(\frac{h-z}{a}+\sqrt{\left(\frac{h-z}{a}\right)^2+4}\right)^{3/2}}\right]. && (7)\\ &E_\theta(r,z) = 0, && (8)\\ &E_z(r,z) \approx \frac{2\sqrt{2}V}{\pi a}\\ &\left[\frac{1}{\sqrt{\left(\frac{h-z}{a}\right)^2+4}\sqrt{\frac{h-z}{a}}\sqrt{\frac{h-z}{a}+\sqrt{\left(\frac{h-z}{a}\right)^2+4}}}+\right. \end{aligned}$$

$$+\frac{1}{\sqrt{\frac{z}{a}}\sqrt{\left(\frac{z}{a}\right)^2+4}\sqrt{\frac{z}{a}+\sqrt{\left(\frac{z}{a}\right)^2+4}}}\Bigg] . \tag{9}$$

Note that for $z \to h$, and $z \to 0$ then $E_r, E_z \to \infty$ (see Figs. 2 and 3).

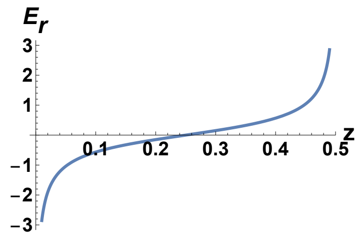

Figure 2: E_r radial component of the electric field $\mathbf{E}$. The positive plate is located at the top. The field is evaluated at the edge of the capacitor, i. e. at $r \approx a$. The parameter values in given unit of length and voltage are: $h = 1/2$, $V_1 = -1$, $V_2 = 1$, $a = 1$, and $r = 0.99$.

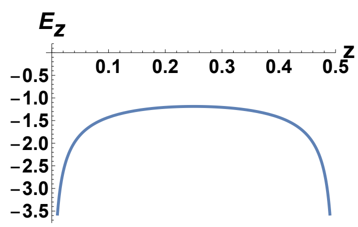

Figure 3: E_z vertical component of the electric field $\mathbf{E}$. The positive plate is located at the top. The field is evaluated at the edge of the capacitor, i. e. at $r \approx a$. The parameter values in given unit of length and voltage are: $h = 1/2$, $V_1 = -1$, $V_2 = 1$, $a = 1$, and $r = 0.99$.

3. Stationary Diffusion in a Finite Domain Driven by an Electric Field

In this section, we propose a statistical model, which describes the ion collision with all the particles inside the cell through a random force $\mathbf{F}$, and the interaction with the electric field during the charge-discharge phase through a deterministic force $q\mathbf{E}$, assuming $q > 0$ in our treatment. At a first approximation, we do not consider the electric field near the ions, since, even if it is very intense close to the particle, it decays quickly. The details of the effect of the electric field in proximity of the ions together with the details of the dendrite formation will be addressed and discussed in Sec. 4, where a simulation model based on a DLA scheme will be considered. Here, we aim at showing that the charged particles in the cell statistically follow the electric field lines, and the probability to find a charged particle in a given region of the cell is determined by the relevant local intensity of the electric field. Due to the fact that the we are considering a finite plate capacitor model for determining the electric field inside the cell, according to the previous section the charge probability distribution is not uniform. This important fact will also be considered in the DLA model of Sec. 4. Let us now start considering the continuity equation

$$\frac{\partial \rho}{\partial t} = -\nabla \cdot \mathbf{J}, \quad \mathbf{J} = \rho \frac{d\mathbf{x}}{dt}, \tag{10}$$

where ρ is the density of the particles, $\mathbf{J}$ is the associated current density and $\mathbf{x} = x\hat{\mathbf{i}} + y\hat{\mathbf{j}} + z\hat{\mathbf{k}}$ is the position vector in a cartesian coordinate system while $\hat{\mathbf{i}}$, $\hat{\mathbf{j}}$ and $\hat{\mathbf{k}}$ are the unit vectors along the x, y and z axes respectively. The equation of motion is

$$m\frac{d^2\mathbf{x}}{dt^2} + \gamma\frac{d\mathbf{x}}{dt} = q\mathbf{E} + \mathbf{F}, \tag{11}$$

where $q\mathbf{E}$ is the deterministic force (electric force) and $\mathbf{F}$ is the stochastic force associated to the collision of the ions with all the particles inside the cell, while m is the mass of the single ion and γ a viscosity coefficient. We will adopt the white noise prescription for $\mathbf{F}$. If we consider the case friction dominated process we may write

$$\frac{d\mathbf{x}}{dt} = q\mu\mathbf{E} + \mathbf{f}, \tag{12}$$

where $\mu = 1/\gamma$ is the mobility and $\mathbf{f} = \mu\mathbf{F}$. Setting $\rho = qn$, the Van Kampen lemma [19] allows us for relating the charged particle density $n(\mathbf{x}, t)$ with the probability density function $P(\mathbf{x}, t)$, i.e.

$$\langle n(\mathbf{x},t)\rangle = P(\mathbf{x},t). \tag{13}$$

Making the statistical average on many density realizations of (10), we have [20]

$$\frac{\partial P(\mathbf{x},t)}{\partial t} = \nabla\cdot(-q\mu\mathbf{E}P(\mathbf{x},t) + D\nabla P(\mathbf{x},t)), \tag{14}$$

where we used (12) for the charged particle velocity $d\mathbf{x}/dt$ and where at the thermodynamical equilibrium it holds $D=\mu kT$ (Einstein's relation, see [20] for its derivation). We may say something in general on the case of a stationary process, i.e. $\partial_t P(\mathbf{x},t)=0$. Considering a closed volume the flowing current has to vanish and we have

$$\begin{aligned} &-q\mu\mathbf{E}P_{eq}(\mathbf{x}) + D\nabla P_{eq}(\mathbf{x}) = \\ &q\mu\nabla\varphi P_{eq}(\mathbf{x}) + D\nabla P_{eq}(\mathbf{x}) = 0, \end{aligned} \tag{15}$$

where P_{eq} is the equilibrium probability distribution. Solving the above equation we obtain the well known solution

$$P_{eq}(\mathbf{x}) = A\exp\left[-q\mu\frac{\varphi}{D}\right] = A\exp\left[-\frac{q\varphi}{kT}\right], \tag{16}$$

where the constant A has to be determined imposing the normalization condition $\int_V P(\mathbf{x},t)dV = 1$. We evaluate the following quantity

$$\begin{aligned} &\frac{P_{eq}(\mathbf{x}_1)}{P_{eq}(\mathbf{x}_2)} = \exp\left[-q\frac{\varphi(\mathbf{x}_1)-\varphi(\mathbf{x}_2)}{kT}\right] \approx \\ &\approx \exp\left[-\frac{q\mathbf{E}(\mathbf{x}_1)\cdot\delta\mathbf{x}}{kT}\right],\ \ \delta\mathbf{x}\equiv\mathbf{x}_2-\mathbf{x}_1. \end{aligned} \tag{17}$$

where the approximation indicates the first term of the Taylor series. Being in our case $q>0$, we infer that the ratio of the two probability densities increase exponentially along the lines of force of the electric field $\mathbf{E}(\mathbf{x})$, i.e. when the angle between $\mathbf{E}(\mathbf{x})$ and $\delta\mathbf{x}$ is zero. We deduce that the probability to find the charged particles is larger along the lines of force, where the field is more intense, i.e., near to the capacitor edges.

In spite of the fact that intuitively we are led to conjecture that the charged particles follow the lines of force of the electric field, (16) shows that the equilibrium probability distribution is a function of the potential energy, which is related to the electric field via the gradient operator.

To be more consistent with the two dimensional numerical simulations performed in Sec. 4, we reduce the three dimensional problem discussed above to a two dimensional analysis with a rectangular domain of sides a and b. The vector $\mathbf{x}$ describing the particle position is now given by $\mathbf{x} = x\hat{\mathbf{i}} + z\hat{\mathbf{k}}$ where $\hat{\mathbf{i}}$ and $\hat{\mathbf{k}}$ are the unit vectors along the x and z axes, respectively, and the left low corner of the rectangle is chosen as the origin of the frame system. For simplicity, we consider a uniform field $\mathbf{E}$. Applying (16) to this particular case, we have

$$P_{eq}(\mathbf{x}) \equiv P_{eq}(x,z) = \frac{q^2 E_x E_z \exp\left[\frac{q(E_x x + E_z z)}{kT}\right]}{k^2T^2\left(1-\exp\left[\frac{qaE_x}{kT}\right]\right)\left(1-\exp\left[\frac{qbE_z}{kT}\right]\right)}, \tag{18}$$

where a and b are the sides of the rectangle. To further simplify the problem, we assume that $\mid q\mathbf{E}\cdot\mathbf{x}/(kT) \mid \ll 1$. Using the Taylor expansion $\exp\left[q\mathbf{E}\cdot\mathbf{x}/(kT)\right] \approx 1 + q\mathbf{E}\cdot\mathbf{x}/(kT) + \cdots$, (18) reads at the first order in $q\mathbf{E}\cdot\mathbf{x}/(kT)$ as:

$$\begin{aligned} P_{eq}(x,z) &\approx \frac{1+\frac{q(E_x x + E_z z)}{kT}}{k^2T^2ab\left[\frac{1}{k^2T^2}+\frac{q(aE_x+bE_z)}{2k^3T^3}\right]} \approx \\ &\frac{1}{ab}\left[1-\frac{q(aE_x+bE_z-2(E_x x+E_z z))}{2kT}\right]. \end{aligned} \tag{19}$$

The probability Pr to find a charged particle in a small rectangle of area $(a_2 - a_1)(b_2 - b_1)$ is

$$\begin{aligned} &Pr\left[a_1 \le x \le a_2, b_1 \le z \le b_2\right] = \int_{\Delta S} P_{eq}(x,z)\,dxdz \approx \\ &\frac{\Delta S}{S}\left[1-\frac{q(a-a_1-a_2)E_x + q(b-b_1-b_2)E_z}{2kT}\right], \end{aligned} \tag{20}$$

where $\Delta S = (a_2 - a_1)(b_2 - b_1)$ and $S = ab$. Note that the first term of the probability, $\Delta S/S$, represents the uniform probability, namely the process without the electric field while the second term represent the small correction to the uniform probability caused by the presence of the electrical field. The corresponding two dimensional expression of (17) for nonuniform electric field distribution writes unchanged as:

$$\frac{P_{eq}(\mathbf{x}_1)}{P_{eq}(\mathbf{x}_2)} = \exp\left[-q\frac{\varphi(\mathbf{x}_1) - \varphi(\mathbf{x}_2)}{kT}\right] \approx \exp\left[-\frac{q\mathbf{E}(\mathbf{x}_1)\cdot\delta\mathbf{x}}{kT}\right], \qquad (21)$$

where we now defined $\delta\mathbf{x} \equiv \mathbf{x}_2 - \mathbf{x}_1 = (x_2 - x_1)\hat{\mathbf{i}} + (z_2 - z_1)\hat{\mathbf{k}}$.

Although the previous discussion is more qualitative than quantitative, it is important to note that if the thermal energy kT is greater than the potential energy $q\varphi$ ($kT \gg q\varphi$) then the presence of the electric field slightly changes the uniform probability to find an ion in a given volume, see (20). If the electrical field is so intense such that $kT \ll q\varphi$ then the charged particles will gather along the electrical field lines where the electric field is more intense. [[With reference to the capacitor under study, as shown in (7) and (9), this condition is realized near the border of the circular plates.]] Using the results of this elementary model we may infer that if it holds the condition $kT \gg q\varphi$, then the charged particles will tend to weakly follow the force lines of the electrical field and their distribution will be almost uniform, see (20). In this case the thermal energy counteracts the charged particle aggregation. If it holds $kT \ll q\varphi$ then the probability density, roughly speaking, is different of zero only along the field lines where the electric field is more intense. This implies that the majority of the ions will gather mostly along such lines, facilitating the aggregation of the charged particles along those lines.

4. DLA Numerical Simulation

The model adopted for the simulation of dendritic growth in our batteries is based on a statistical DLA (Diffusion Limited Aggregation) scheme, which is a model proposed by Witten and Sander in 1981 to explain the observed fractal shape of dust particle aggregates [11]. The traditional DLA simulation starts with an initial seed particle positioned at the center of an $m \times n$ matrix and another particle in some other part of the lattice, free to move following a random walk due to Brownian motion, until it reaches the seed particle and aggregates with it. Subsequent released particles follow the same diffusion process until they aggregate to form a cluster centered on the seed particle.

In our case, the DLA simulation is obtained by allowing the random walkers to initially aggregate to a straight line of seed particles positioned at the bottom of the $m \times n$ matrix. For the sake of clarity, the matrix $m \times n$ represents the rectangle of sides a and b mentioned in Sec. 3, which models the two dimensional space between the two electrodes of the cell. The randomness of the diffusion process of our model is biased by an anisotropic probability distribution of movement of the free particles to favor their movement in some directions rather than others. In more detail, we partition the $m \times n$ matrix in k configurable zones, each having a specific set of probability values for the free particle to move up, down, left, or right during its diffusion process. At the same time, to mimic the conservation of the number of particles, every time a diffusing particle (representing an ion in our case) reaches one of the two sides, or the top, of the $m \times n$ matrix it bounces off and it continues its random walk. With these choices, we are able to represent:

a) The space between the electrodes of our cells with the matrix $m \times n$;

b) The variable electric field between the electrodes with the k probability zones.

In Figs. 4 and 5, we show the results of a simulation of an $m \times m$ matrix in the case of 49 zones of isotropic and anisotropic probability distribution of movement of the free particles, respectively.

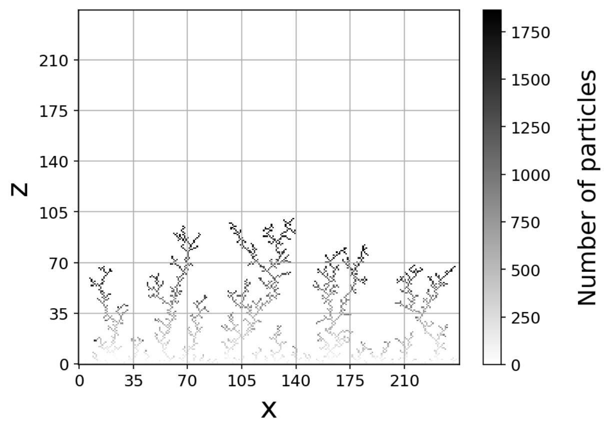

Figure 4: Simulation of a 245×245 matrix with 49 zones of isotropic probability distribution of movement. Aggregation of 1864 particles.

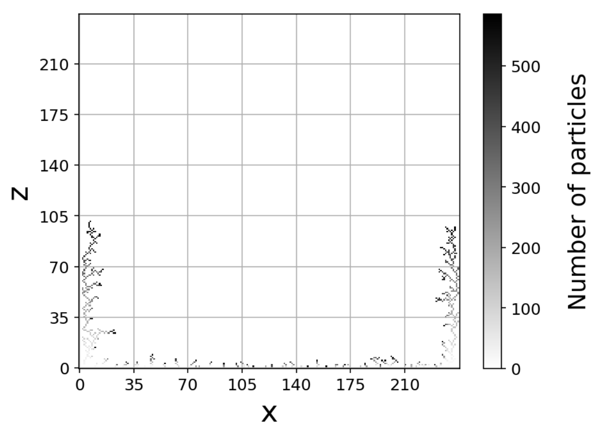

Figure 5: Simulation of a 245×245 matrix with 49 zones of anisotropic probability distribution of movement. Aggregation of 586 particles.

In order to keep the growth of the dendrites in reasonable simulation times, we decided to end the simulation half way between the two electrodes. The probability distribution of movement of the free particles has been selected accordingly to the intensity of the electric field. In more detail, the probability distribution increases moving towards the down-right and down-left corner.

The program for this simulation was developed using the free and opensource Anaconda distribution, which includes Python 3.6 and all the up-to-date scientific packages that come with it.

5. Conclusions

We presented a new model of dendrite growth in battery cells. Through a statistical model, we described how the deterministic electric field and the stochastic force combine to drive the charged particles inside the battery cell. We simulated the dendrite growth via Diffusion Limited Aggregation model for different electric field distributions inside the cell. Finally, we showed how charged particles align along the intense electric field, thus making critical for the growth of dendrites the region close to the edges of the electrodes.

Acknowledgements

This work was supported by the PROT-ONE Project, FAR-FAS 2014, CUP 4421.02102014.07200099, funded by Regione Toscana.

[1] R. Akolkar, "Mathematical model of the dendritic growth during lithium electrodeposition," Journal of Power Sources, 2013, vol. 232, p. 23-28.

[2] L. Kong, Y. Xing, and M. G. Pecht, "In-Situ Observations of Lithium Dendrite Growth," IEEE Access, 2018, vol. 6, p. 8387-8393.

[3] I. W. Seong, C. H. Hong, B. K. Kim, W. Y. Yoon, "The effects of current density and amount of discharge on dendrite formation in the lithium powder anode electrode," Journal of Power Sources, 2008, vol. 178, p. 769-773.

[4] F. Sagane, K. Ikeda, K. Okita, H. Sano, H. Sakaebe, Y. Iriyama, "Effects of current densities on the lithium plating morphology at a lithium phosphorus oxynitride glass electrolyte/copper thin film interface," Journal of Power Sources, 2013, vol. 233, p. 34-42.

[5] Y. Cui, C. L. Xu, Q. Y. Han, H. Choo, P. K. Liaw, "Formation of dendritic nanotubes under an electric field," Advanced Engineering Materials, 2005, vol. 7, no. 9, p. 827-829.

[6] A. Jana, D. R. Ely, R. E García, "Dendrite-separator interactions in lithium-based batteries," Journal of Power Sources, 2015, vol. 275, p. 912-921.

[7] P. Zou, Y. Wang, S.-W. Chiang, X. Wang, F. Kang, C. Yang, "Directing lateral growth of lithium dendrites in micro-compartmented anode arrays for safe lithium metal batteries," Nature Communications, 2018, vol. 9:464, p. 1-9.

[8] M. M. Rezinkina, "Modeling of the Dendrite Shape Variation with Applied Electric Field Strength in Poly(ethylene)," Technical Physics Letters, 2000, vol. 26, no. 3, p. 196-198.

[9] A. Aryanfar, D. Brooks, B. V. Merinov, W. A. Goddard, III, A. J. Colussi, and M. R. Hoffmann, "Dynamics of Lithium Dendrite Growth and Inhibition: Pulse Charging Experiments and Monte Carlo Calculations," J. Phys. Chem. Lett., 2014, vol. 5, p. 1721-1726.

[10] M. S. Park, S. B. Ma, D. J. Lee, D. Im, S.-G. Doo, O. Yamamoto, "A Highly Reversible Lithium Metal Anode," Scientific Reports, 2014, vol. 4, p. 1-8.

[11] T. A. Witten, L. M. Sander, "Diffusion-limited aggregation, a kinetic critical phenomenon," Phys. Rev. Lett. 1981, 47(19), p. 1400-1403.

[12] C. Lupo and D. Schlettwein, "Modeling of Dendrite Formation as a Consequence of Diffusion-Limited Electrodeposition," J. Electrochem. Soc., 2019, vol. 166, no. 1, p. D3182-D3189.

[13] J. E. Guyer, W. J. Boettinger, and J. A. Warren, "Phase field modeling of electrochemistry. I. Equilibrium," Phys. Rev. E, 2004, vol. 69, p. 021603-1-13.

[14] L. D. Landau, L. P. Pitaevskii and E. M. Lifshitz, “Electrodynamics of Continuous Media”, 2nd ed. Elsevier Butterworth-Heinemann, Oxford (1984).

[15] J. D. Wiley, J. G. Webster, “Analysis and Control of the Current Distribution under Circular Dispersive Electrodes,” IEEE Trans. Biomedical Eng., 1982, vol. BME-29, no. 5, p. 381-385.

[16] K. Nisancioglu, J. Newman, “The short-time response of a disk electrode,” J. Electrochem. Soc., 1974, vol. 121, p. 523527.

[17] H. Lee, S. Chen, X. Ren, A. Martinez, V. Shutthanandan, M. Vijayakumar, K. Sung Han, Q. Li, J. Liu, W. Xu, and J.-G. Zhang, “Electrode Edge Effects and the Failure Mechanism of Lithium-Metal Batteries,” ChemSusChem, 2018, vol. 11, p. 3821-3828.

[18] W. Yu, “Fractal Properties and Applications of Dendritic Filaments in Programmable Metallization Cells,” PhD Thesys, Arizona State University, Dec. 2015.

[19] N. G. Van Kampen, Phys. Rep. vol. 24, 171, 1976.

[20] R. Kubo, M. Toda and N. Hashitsume, “Statistical Physics II Nonequilibrium Statistical Mechanics”, 3rd ed. Springer, Berlin (1991).